Separation Science and Technology
Publication details, including instructions for authors and subscription information:
http://www.informaworld.com/smpp/title~content=t713708471

Longitudinal Distribution of pH in Preparative Electrophoresis in a Multicompartment Electrolyzer

Jin Wang[a]; Zheng Liu[a]; Fuxin Ding[a]; Naiju Yuan[a]
[a] DEPARTMENT OF CHEMICAL ENGINEERING, TSINGHUA UNIVERSITY, BEIJING, PEOPLE'S REPUBLIC OF CHINA

To cite this Article Wang, Jin , Liu, Zheng , Ding, Fuxin and Yuan, Naiju(1999) 'Longitudinal Distribution of pH in Preparative Electrophoresis in a Multicompartment Electrolyzer', Separation Science and Technology, 34: 8, 1661 — 1677
To link to this Article: DOI: 10.1080/01496399909353763
URL: http://dx.doi.org/10.1080/01496399909353763

SEPARATION SCIENCE AND TECHNOLOGY, **34**(8), pp. 1661–1677, 1999

Longitudinal Distribution of pH in Preparative Electrophoresis in a Multicompartment Electrolyzer

JIN WANG, ZHENG LIU,* FUXIN DING, and NAIJU YUAN
DEPARTMENT OF CHEMICAL ENGINEERING
TSINGHUA UNIVERSITY
BEIJING 100084, PEOPLE'S REPUBLIC OF CHINA

ABSTRACT

Generating an expected longitudinal pH distribution is of essential importance for achieving high resolution in an electrophoresis process conducted in a multicompartment electrolyzer. A simulation of the longitudinal distribution of pH in a multicompartment electrolyzer is proposed on the basis of mass transfer analysis and electrolysis equilibrium of the electrolytes. Selection of the operating conditions to establish an expected pH distribution with a conventional electrolyte rather than an ampholyte can thus be accomplished according to the simulation results. Numerical solution of this model is developed on the basis of the Gear method. The calculated results agree well with the experimental data in a wide range of operation conditions including applied potential, sample loading flow rate, and protein concentration in solution. This model may also be applied to other ampholyte-free electrophoresis processes conducted in a membrane-spaced multicompartment electrolyzer.

Key Words. Electrophoresis; Multichannel flow electrophoresis; Multicompartment electrolyzer; pH gradient

*To whom correspondence should be addressed. Telephone: 86-10-6278-5534. FAX: 86-10-6277-0304. E-mail: liuzheng@tsinghua.edu.cn

INTRODUCTION

Scaling up electrophoresis for the large-scale separation of biological molecules has been attempted for decades with emphasis on the dissipation of Joule heating and eliminating the mixing of product streams. Of the methods and apparatuses developed to date, conducting electrophoresis in a multicompartment electrolyzer, as shown by multichannel flow electrophoresis (1), recycling isoelectric focusing (2), and immobilized pH gradient multicompartment isoelectric focusing (3), has proven to be effective in eliminating the mixing of product streams caused by either hydrodynamic instability or Joule heating. It is thus possible to apply a high potential in electrophoresis to achieve a high throughput and a high resolution as well.

Multichannel flow electrophoresis (MFE) is a newly developed preparative electrophoresis method employing a membrane-partitioned 5-compartment electrolyzer (1). During a run, the protein mixture is continuously introduced into the central compartment. The charged components are transmitted into the neighboring elution compartments and washed out by carrier flow, while the neutral component and the weakly charged components are carried out of the central compartment by sample flow. Various separation strategies are available for MFE through different choices of the buffering pH, which can be conveniently accomplished by a suitable selection of buffering ions used for preparing the sample solution and elution carrier. For example, by setting the pH of the buffer identical to the isoelectric point of the target component, the charged impurities can be carried into the washing compartment while the target component is carried out through the central compartment. For separation of a binary protein mixture, the pH of the buffer could be set at a value between the isoelectric points of the components in order to obtained two oppositely charged components simultaneously from their corresponding elution compartment.

In the electrophoresis process conducted in a multicompartment electrolyzer, the fluid in each compartment changes its pH value along the flow axis as the result of ion migration among the fluid in neighboring compartments. Maintaining a uniform longitudinal distribution of pH along the flow direction in the central compartment is a key to maintaining the desired charges of the target component and the impurities and, consequently, to achieving the expected separation. In a conventional isoelectric focusing process conducted in a multicompartment electrolyzer, the expected pH distribution is generated and maintained by adding ampholyte to the mixture solution, as shown by recycle isoelectric focusing (2). However, the high operating cost and the requirement of complete removal of ampholyte from the product solution for safety reasons make this method unsuitable for large-scale separations.

Since the longitudinal pH distribution, as shown later in this paper, is a function of the applied potential, buffer composition, and the liquid flow rate in each compartment, an expected pH distribution can be obtained and maintained by a proper selection of these operations parameters. On the basis of mass conservation, electrolysis equilibrium of the electrolytes, and electric neutrality in a compartment, a simulation of the pH distribution can be established. Selection of suitable conditions for a given separation task can thus be accomplished based on the numerical solution of this model. This model could also be applied to other electrophoresis processes employing multicompartments in the absence of ampholyte, such as forced flow electrophoresis (4) and electric split-flow fractionation (5) due to their similarity in ion and protein transfer in electrophoresis process.

In this article a mathematical model is proposed on the basis of above considerations. A numerical solution is developed on the basis of the Gear method (6). The accuracy of this model has been tested experimentally using Tris–HAc buffer and bovine serum albumin as a sample system.

MATHEMATICAL APPROACHES

Mass Transfer Analysis

For an element taken from a compartment, as shown in Fig. 1, the mass transfer along the direction of the electric field is contributed to by

1. Electrophoretic migration of ions
2. Molecular diffusion by concentration gradient
3. Migration flux driven by hydraulic pressure
4. Electroosmosis
5. Thermodiffusion

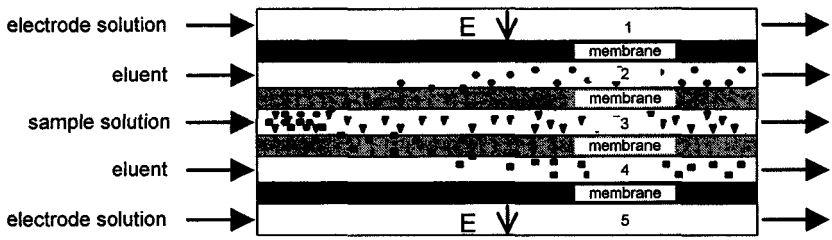

FIG. 1 Schematic view of the separation process of the MFE.

The mass transfer along the flow axis is contributed to by

1. Mass transfer carried out by fluid flow
2. Molecular diffusion by concentration gradient
3. Thermodiffusion
4. Migration introduced by steaming potential

Similarly, for an element taken from the membrane, the mass transfer processes along the direction of the electric field are

1. Electrophoretic migration
2. Molecular diffusion caused by concentration gradient
3. Electroosmosis
4. Thermodiffusion

In the meantime, the mass transfer inside the membrane along the direction perpendicular to the electric field is contributed to by

1. Molecular diffusion
2. Thermodiffusion

For a microfiltration (MF) membrane partitioned multicompartment electrolyzer, the accumulations of proteins and ions inside the membrane can be neglected due to the large pore size and high porosity of the MF membrane. In MFE, the gel membrane was used to separate the elution compartment and electrode compartment, which showed little resistance to ion transportation. For a continuous mode of operation, a steady longitudinal distribution of pH gradient in each compartment can be reached.

Mathematical Modeling

Based on experimental studies on MFE, the above physical model can be rationally simplified by omitting those elements contributing little to mass transfer. Therefore, a mathematical model describing the longitudinal distribution can be established.

Assuming that:

1. The flow pattern in each compartment is an ideal plug flow
2. The mass transfer contributed by diffusion processes and by steaming potential can be omitted compared with that carried out by fluid flow
3. The mass transfer along the electric axis contributed by diffusion processes can be ignored compared with that contributed by electrophoretic migration and electroosmosis
4. The electroosmosis flux is prevented, and thus makes no contribution to ion transportation
5. The contribution to pH changes by the biological molecules present in dilute form can be omitted

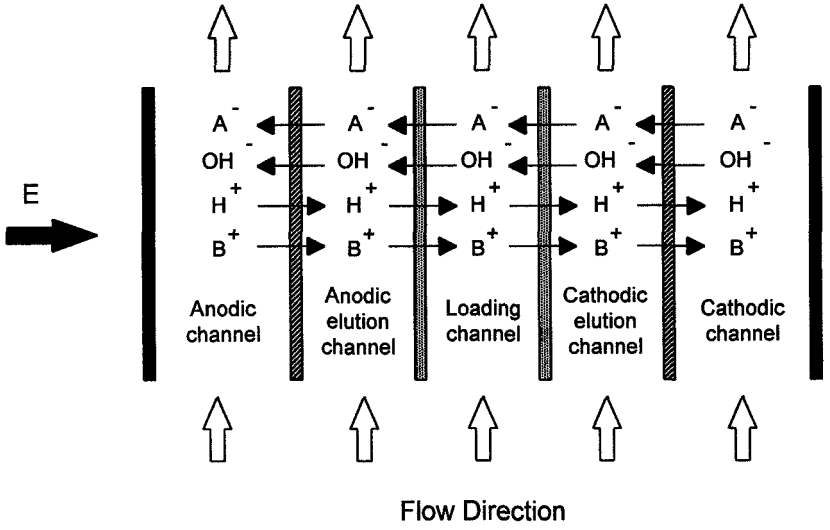

FIG. 2 Simplified model of the mass transfer in the MFE process.

Based on the above assumptions, a two-dimensional distribution of the pH gradient can be established.

Taking a simple buffer composed of a weak acid HA and a weak base BOH as an example, the migration of the ions described above is as shown in Fig. 2.

For a thin layer taken from a compartment along the flow direction, as shown in Fig. 3, and based on the above analysis of mass transfer processes,

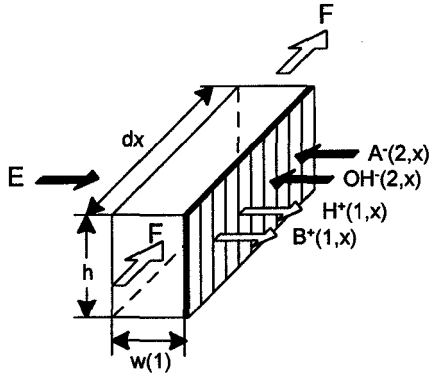

FIG. 3 Mass transfer in the anode compartment.

equations of electrophoretic migration, mass conservation, and neutrality of the element can be established. For the anode compartment, the equations are as follows.

The residence time of the fluid in the element is

$$dt(1) = h \cdot w(1) \cdot dx / v(1) \tag{1}$$

The amount of anion A introduced from the neighboring anodic elution compartment is

$$dm_{A^-}(1,x) = \mu^{\circ}_{A^-} \cdot \frac{U(2)}{w(2)} \cdot C_{A^-}(2,x) \cdot h \cdot dx \cdot dt(1) \tag{2}$$

The amount of cation B^+ migrated to the anode compartment is

$$dm_{B^+}(1,x) = -\mu^{\circ}_{B^+} \frac{U(1)}{w(1)} \cdot C_{B^+}(1,x) \cdot h \cdot dx \cdot dt(1) \tag{3}$$

Due to the fact that current density in electrophoresis is usually controlled at a level of 0.5 mA, electrolysis at the electrode contributes little to the concentration changes of H^+ and OH^-. Furthermore, H^+ and OH^- concentrations are generally much smaller than B^+ and A^- in the buffer. Therefore, transportation of H^+ and OH^- is excluded in the following transport equations.

For HA and BOH, the changes of mass caused by the corresponding transfer of ions are

$$dm_A(1,x) = -dm_{A^-}(1,x)$$

$$dm_B(1,x) = -dm_{B^+}(1,x)$$

The concentrations of A and B can be expressed as functions of A^- and B^+ based on their corresponding electrolysis equilibrium. Introducing these expressions into Eqs. (2) and (3) gives

$$\frac{dC_A(1,x)}{dx} = \mu_{A^-} \frac{U(2)}{w(2)} \cdot \frac{k_a C_A(2,x)}{k_a + C_{H^+}(2,x)} \cdot \frac{h}{v(1)} \tag{4}$$

$$\frac{dC_B(1,x)}{dx} = -\mu^{\circ}_{B^-} \cdot \frac{U(1)}{w(1)} \cdot \frac{k_b C_B(1,x) C_{H^+}(1,x)}{k_w + k_b C_{H^+}(1,x)} \cdot \frac{h}{v(1)} \tag{5}$$

Electric neutrality requires

$$\frac{k_a C_A(1,x)}{k_a + C_{H^+}(1,x)} + \frac{k_w}{C_{H^+}(1,x)} - C_{H^+}(1,x) - \frac{k_b C_B(1,x) C_{H^+}(1,x)}{k_w + k_b C_{H^+}(1,x)} = 0 \tag{6}$$

The initial conditions are

$$C_A(1,0) = C_{A0}$$
$$C_B(1,0) = C_{B0} \tag{7}$$
$$C_{H^+}(1,0) = C_{H^+0}$$

Similarly, for the anodic elution compartment, the sample loading compartment, the cathodic elution compartment, and the cathode compartment, there are

$$\frac{dC_A(1,x)}{dx} = \mu_{A^-}\frac{U(2)}{w(2)} \cdot \frac{k_a C_A(2,x)}{k_a + C_{H^+}(2,x)} \cdot \frac{h}{v(1)} \tag{8}$$

$$\frac{dC_A(i,x)}{dx} = \mu_{A^-}\left[\frac{U(i+1)}{w(i+1)} \cdot \frac{k_a C_A(i+1,x)}{k_a + C_{H^+}(i+1,x)} - \frac{U(i)}{w(i)} \cdot \frac{k_a C_A(i,x)}{k_a + C_{H^+}(i,x)}\right] \frac{h}{v(i)}, \qquad i = 2, 3, 4 \tag{9}$$

$$\frac{dC_A(5,x)}{dx} = -\mu_{A^-}\frac{U(5)}{w(5)} \cdot \frac{k_a C_A(5,x)}{k_a + C_{H^+}(5,x)} \cdot \frac{h}{v(5)} \tag{10}$$

$$\frac{dC_B(1,x)}{dx} = -\mu_{B^+}\frac{U(1)}{w(1)} \cdot \frac{k_b C_B(1,x) C_{H^+}(1,x)}{k_w + k_b C_{H^+}(1,x)} \cdot \frac{h}{v(1)} \tag{11}$$

$$\frac{dC_B(i,x)}{dx} = -\mu_{B^+}\left[\frac{U(i-1)}{w(i-1)} \frac{k_b C_B(i-1,x) C_{H^+}(i-1,x)}{k_w + k_b C_{H^+}(i-1,x)} - \frac{U(i)}{w(i)} \cdot \frac{k_b C_B(i,x) C_{H^+}(i,x)}{k_w + k_b C_{H^+}(i,x)}\right] \cdot \frac{h}{v(i)}, \qquad i = 2, 3, 4 \tag{12}$$

$$\frac{dC_B(5,x)}{dx} = \mu_{B^+}\frac{U(4)}{w(4)} \cdot \frac{k_b C_B(4,x) C_{H^+}(4,x)}{k_w + k_b C_{H^+}(4,x)} \cdot \frac{h}{v(5)} \tag{13}$$

$$\frac{k_a C_A(i,x)}{k_a + C_{H^+}(i,x)} + \frac{k_w}{C_{H^+}(i,x)} - C_{H^+}(i,x) - \frac{k_b C_B(i,x) C_{H^+}(i,x)}{k_w + k_b C_{H^+}(i,x)} = 0, \qquad i = 1, 2, \ldots, 5 \tag{14}$$

The initial conditions are:

$$C_A(i,0) = C_{A0}, \qquad i = 1, 2, \ldots, 5$$
$$C_B(i,0) = C_{B0}, \qquad i = 1, 2, \ldots, 5 \tag{15}$$
$$C_{H^+}(i,0) = C_{H^+0}, \qquad i = 1, 2, \ldots, 5$$

To get rid of the effects of the generation and emission of H_2 and O_2 bubbles resulting from electrolysis in the cathode and anode compartments, re-

spectively, on the determination of the voltage drop in each compartment, MFE was conducted in a constant current density mode. Therefore, the voltage applied to each compartment can be calculated on the basis of Ohm's law as

$$U(i) = \frac{I \cdot h(i)}{l(i \cdot w(i) \cdot \kappa} \tag{16}$$

in which I is the current density, and $h(i)$, $l(i)$, and $w(i)$ are the dimensions shown in Fig. 3. It should be noted here that the existence of gas bubbles in the electrode compartments may lead to an error in the determination of the voltage of these two compartments according to Eq. (16). However, this error can be ignored because it contributes little to the determination of the pH changes in the electrode compartment due to the rapid circulation of carrier flow inside the electrode compartments.

In addition, ion transfer in the electrophoresis process leads to a change in ion concentration in each compartment. A corresponding change of the applied potential to each compartment occurs and maintains a constant current density across each compartment. The potential drop in each compartment can be expressed as

$$U(i,x) = \alpha(i,x) \cdot U(i,0), \qquad i = 1, 2, ..., 5 \tag{17}$$

in which $\alpha(1,x) = \alpha(5,x) = 1.0$. This is because the amount of ions transported from the elution compartment to the electrode compartment can be omitted compared to the total amount of the ions carried through the electrode compartments by rapid liquid circulation. The ionic strength in the electrode compartments can thus be assumed to be constant. Therefore, the potential drops in the electrode compartments can also be assumed to be constants when electrophoresis is conducted in a constant current density operation mode.

The current density across each membrane is

$$e(i) = \mu_{A^-} \frac{\alpha(i+1,x)U(i+1)}{w(i+1)} \cdot \frac{k_a C_A(i+1,x)}{k_a + C_{H^+}(i+1,x)} + \mu_{B^+} \frac{U(i)}{w(i)} \cdot \frac{k_b C_B(i,x) C_{H^+}(i,x)}{k_w + k_b C_{H^+}(i,x)}, \qquad i = 1, 2, \ldots, 4 \tag{18}$$

When electrophoresis conducted in a constant current density mode, then

$$e(i) = e(i+1), \qquad i = 1, 2, \ldots, 4 \tag{19}$$

Numerical Solution of the Model

The calculating diagram is shown as Fig. 4. During the integration of dif-

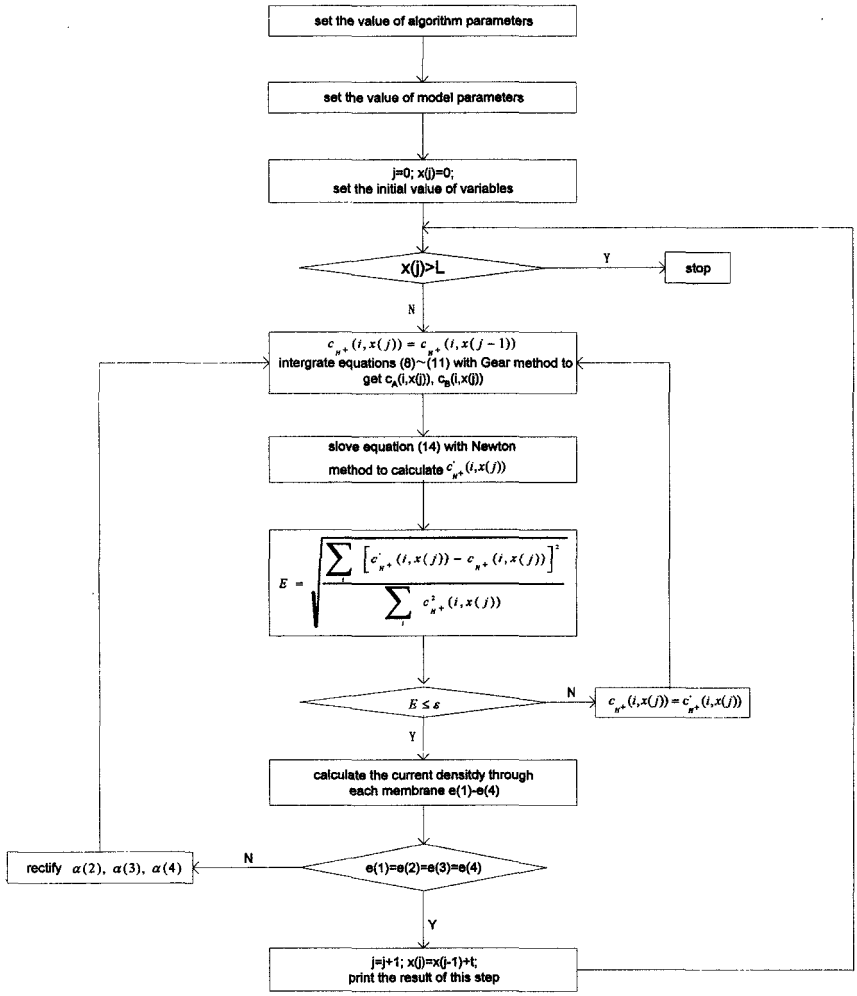

FIG. 4 Block diagram of the algorithm.

ferential equation groups, the nondifferential variables which also appear in the algebraic equations were regarded as constant, and their initial values were set as their value in the last node. Then the solution obtained from the differential equations was introduced into the algebraic equations. The second value of the nondifferential variables was thus obtained. By setting the second value as the initial value of the nondifferential variables and repeating the above procedure until the difference between the sequential value of the non-

differential variables is within the given range, one step of the integration is finished.

EXPERIMENTAL

The MFE apparatus was the same as that shown in Ref. 1. In this work, HT Tuffryn, a kind of hydrophilic polysulfone microfiltration membrane (pore size: 0.45 μm) (8), was placed between the central compartment and the elution compartment. The elution compartments and the electrode compartments were spaced by a gel membrane synthesized according to Yuan's patent (7). Each compartment was connected to its own pump. All compartments were 120.00 mm in length and 10.00 mm in width. The depth were 4.02 mm for the anode compartment, 4.10 mm for the cathode compartment, 2.84 mm for the two elution compartments, and 2.80 mm for the central compartment.

During a run the protein sample solution was continuously pumped into the central compartment, while the washing carriers were pumped into the elution compartments and the electrode compartments, respectively. The separated component was then collected at the outlet of its corresponding compartment. The washing carriers of electrode compartments were collected, mixed, and recycled after degasing. After the experiment a reverse electric field was applied by altering the cathode and anode to remove the protein adsorbed on the membrane in order to regenerate the system for a subsequent run.

RESULTS AND DISCUSSIONS

0.01 M Tris–HAc was applied in the experimental studies of this paper. The pH of the buffer varied between 5.90 to 6.20. The temperature was maintained at 10°C. Current densities were maintained at 20, 40, 60, and 80 mA, respectively. The sample loading flow rates were 2, 3, 4, and 5 mL/min. The mobility is 28.27 $cm^2 \cdot s^{-1} \cdot V^{-1}$ for Ac^- and 20.20 $cm^2 \cdot s^{-1} \cdot V^{-1}$ for $Tris^+$ (9).

Calculated Longitudinal Distributions of pH in Each Compartment

To illustrate the effects of applied potential and buffer flow rate on the longitudinal pH distribution in each compartment, a calculated pH distribution in each compartment is presented in Fig. 5–7 for a flow rate of the central compartment of 1.0 mL/min and ratios of the flow rate in the central compartment to that of the elution compartment of 1:1, 1:1.5, and 1:2, respectively.

These figures show that the longitudinal pH distribution in each compartment is a function of the applied potential, as indicated by the current density, and of the buffer flow rate. In all cases, the higher the applied potential, the larger the pH along the flow direction, as indicated by the difference between

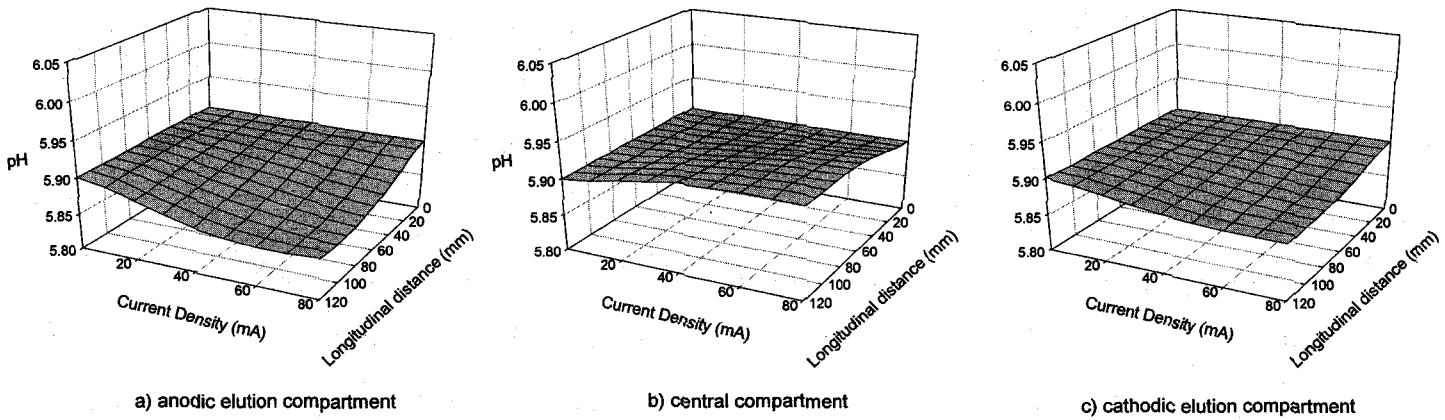

FIG. 5 Calculated longitudinal distribution of pH as a function of applied potential and flow rate in each compartment. (The flow rate is 1.0 mL/min for the central compartment and 1.0 mL/min for the elution compartments.)

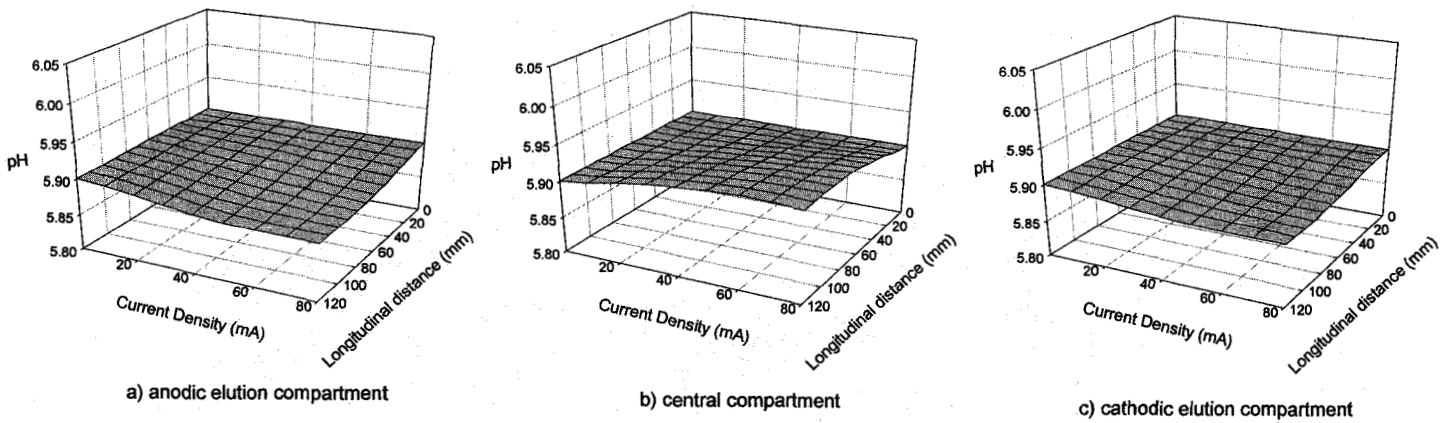

FIG. 6 Calculated longitudinal distribution of pH as a function of applied potential and flow rate in each compartment. (The flow rate is 1.0 mL/min for the central compartment and 1.5 mL/min for the elution compartments.)

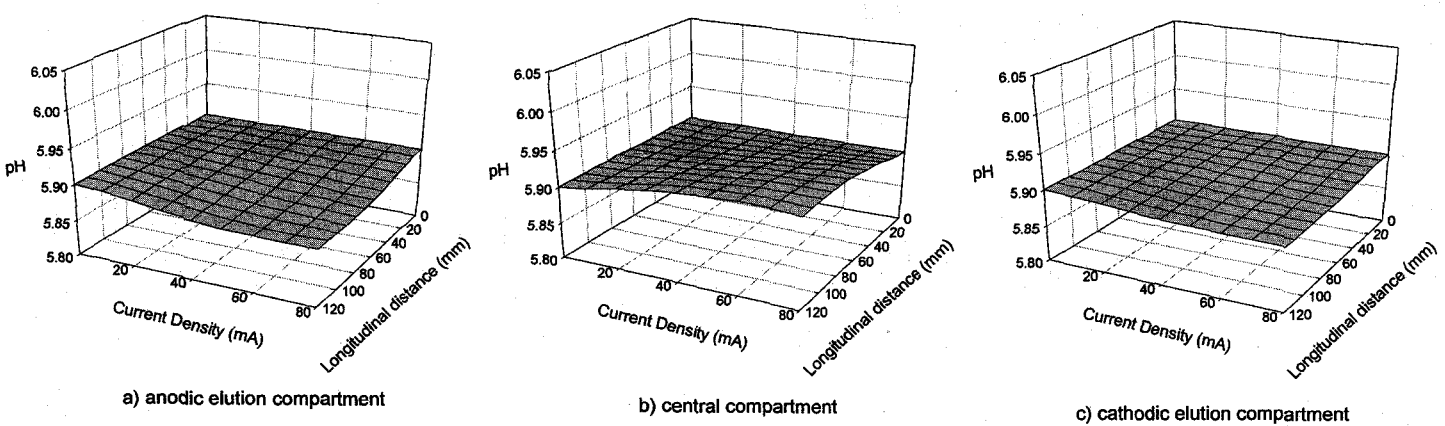

FIG. 7 Calculated longitudinal distribution of pH as a function of applied potential and flow rate in each compartment. (The flow rate is 1.0 mL/min for the central compartment and 2.0 mL/min for the elution compartments.)

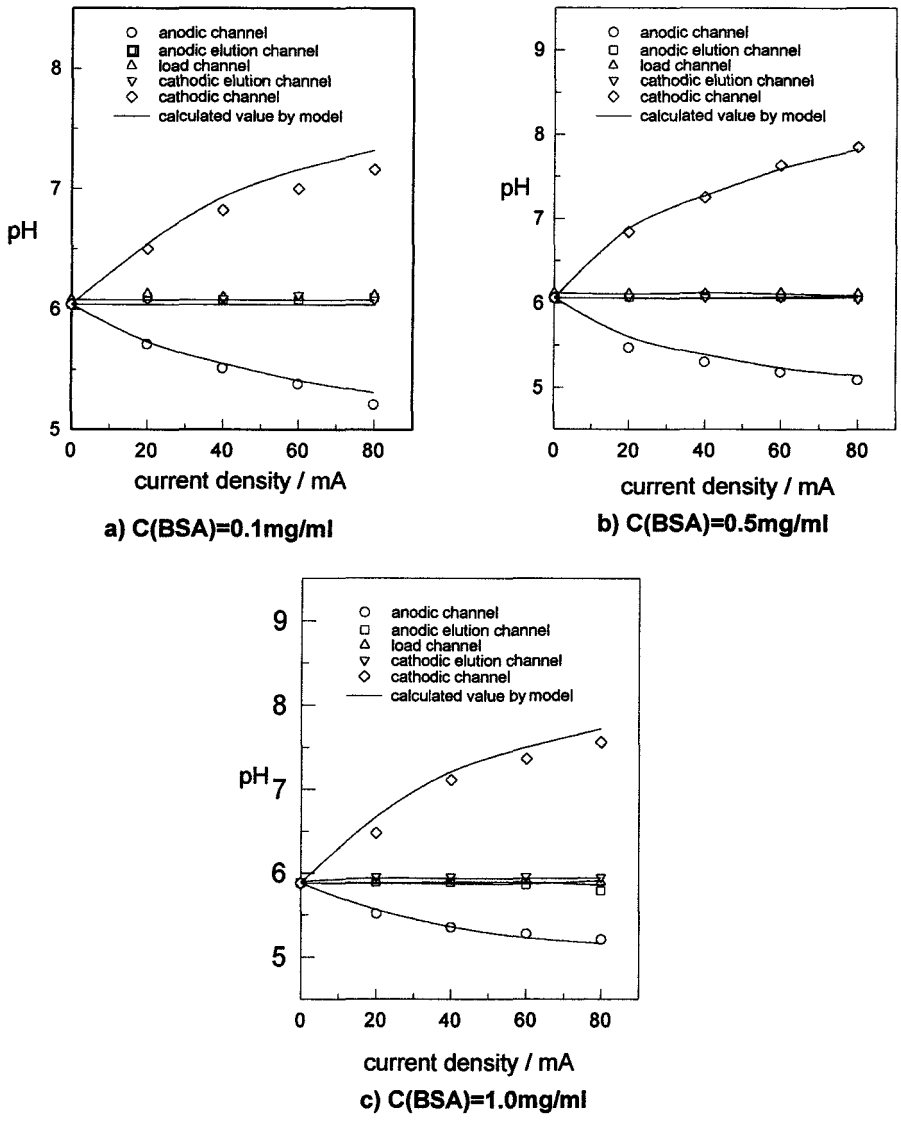

FIG. 8 Comparison of the experimental and the calculated pH longitudinal distribution.

pH values at the inlet and the outlet of each compartment. The increase of the flow rate in the elution compartment leads to a tiny increase in the pH shift in the central compartment but to a slightly greater reduction in the pH shift in the elution compartment.

In all cases, the pH shifts along the flow direction fall into quite a narrow

range. This is mainly due to the approachable electrophoretic mobility of $Tris^+$ and Ac^-. It is also noteworthy that the change of pH in the central compartment is much smaller than in the elution compartments, a result of the symmetrical nature of ion transfer. This essentially ensures the high resolution of the electrophoresis.

In general, the selection of buffering ions depends on the separation sought, while the applied potential is determined by the heat-exchange capacity of the apparatus. The maximum flow rate in the central compartment is that at which the charged component is given adequate residence time to be fully removed from the central compartment. Meanwhile, the minimum flow rate of the buffer in the elution compartment is that at which the polarity is not altered. In this way the selection of a suitable fluid flow rate in each compartment can be determined on the basis of simulation results. This makes the optimization effective and economic, especially when large-scale separation is dealt with.

Experimental Validation of the pH Model Using BSA Solution

An experimental demonstration of this model was conducted using BSA dissolved in 0.01 M Tris–HAc buffer as the sample; Tris–HAc was also applied as the washing carrier. In the experiments the sample loading flow rate and the washing buffer flow rate were maintained at 2 and 3 mL/min, respectively. The BSA concentration was sequentially changed from 0.1 to 0.5 to 1.0 mg/mL.

The calculated data and the experimental results are shown in Fig. 8, respectively. In all cases the calculated data agree well with the experiment data obtained in the central compartment and elution compartments. A relatively larger error was observed in the electrode compartments, especially in the anode compartment. This is because the fluid flow rate varied due to the presence of gas bubbles in the experiments. The divergence of pH value in the electrode compartments during recycling also contributed to the error. For the central compartment and the elution compartments, the maximum error of the calculated results is 3.4%. This demonstrates the reliability of the proposed model.

CONCLUSIONS

For the electrophoretic separation of biological molecules based on their charges, establishing and maintaining an expected pH gradient is of essential importance for the success of separation. With respect to the electrophoresis processes in a multicompartment electrolyzer, as shown by present work, it is possible to generate an expected pH distribution through a suitable choice of operating conditions including applied potential, fluid flow rate in each compartment and of buffer ions, etc.

It should be pointed out that in present work the main interest is to generate a uniform longitudinal distribution in the central compartment where separation of a protein mixture is conducted. This is different from multicompartment isoelectric focusing processes where a pH gradient along the electric field is required. Therefore, it is suitable to apply the MFE for the productive separation of one target component in a mixture. Application of this technique for analytical purposes where all components are to be separated is not recommended. The productive recovery of more than one component from a mixture may be accomplished with a series of MFE processes, each of which is operated at a suitable pH for the recovery of one product.

As indicated by the present study, in such a preparative electrophoresis process the contribution of proteins to current density can be neglected. This is demonstrated by the fairly good agreement between the calculated data and the experimental results obtained in a wide range of operating conditions when protein concentration is maintained at a low level, e.g., below 1 mg/mL. This model can be applied for large-scale electrophoresis dealing with dilute protein solutions.

In large-scale electrophoresis, besides such optional factors as flow pattern, hydraulic mixing, and thermal diffusion, electroosmosis is an important factor that affects the longitudinal distribution of pH. In a membrane-spaced electrolyzer the mass transfer contributed by electroosmosis between neighboring compartment is much more significant in some cases than that contributed by electrophoresis. In present study, electroosmosis flux is eliminated by pressure compensation in each compartment. This is accomplished by adding an extra flow resistance to the compartment which is benefited from electroosmosis. In the case where electroosmosis is not fully eliminated, mass transfer caused by electroosmosis along the direction of the electric field should be included in the model presented above. The effect of electroosmosis on large-scale electrophoresis is now being investigated by our group.

ACKNOWLEDGMENTS

Support from the China National Nature Science Foundation (Project 29676022) and the State Department of Science and Technology, People's Republic of China (Project 96C-03-04-05) are gratefully acknowledged. The authors thank Mr. Dongsheng Li for his great efforts at the early stage of this work. The authors also extend their grateful thanks to Mr. Yin Zhao and Mr. Jian Luo for their assistance in the experimental work.

REFERENCES

1. Z. Liu, Z. Huang, J.-Y. Chong, et al., *Sep. Sci. Technol.*, *31*(10), 1427 (1996).

2. M. Bier and N. B. Egrn., in *Developments in Biochemistry*, *Vol. 7* (Haglund et al., Eds.), Elservier-North Holland, Amsterdam, 1979.
3. P. G. Regetti, *J. Chromatogr.*, *500*, 681–696 (1990).
4. S. Levin, M. N. Myers, and J. C. Giddings, *Sep. Sci. Technol.*, *24*, 1245 (1989).
5. M. Bier, T. Long, and H. W. Ryu, *Ibid.*, *25*, 997 (1990).
6. C. W. Gear, *Numerical Initial Value Problems in Ordinary Differential Equations*, Prentice-Hall, Englewood Cliffs, NJ, 1971.
7. N.-J. Yuan, Z. Liu, D.-Q. Zhu, and F.-X. Ding, China Patent 93108630.2.
8. Gelman Sciences brochure, 1996.
9. Z. Liu, Dissertation for Doctor Degree, Tsinghua University, Beijing, People's Republic of China, 1993.

Received by editor April 15, 1998
Revision received October 1998